Modeling of Isochronal Complex Magnetic Susceptibility of Polymer–Magnetic Nanocomposites Using Fractional Calculus

M. A. Garza-Navarro,[1,2] M. E. Reyes-Melo,[1,2] V. González-González,[1,2] C. Guerrero-Salazar,[1,2] U. Ortiz-Méndez[1,2]

[1]*Doctorado en Ingeniería de Materiales, Facultad de Ingeniería Mecánica y Eléctrica, Universidad Autónoma de Nuevo León, San Nicolás de los Garza, Nuevo León 66450, México*
[2]*Centro de Innovación, Investigación y Desarrollo en Ingeniería y Tecnología, Universidad Autónoma de Nuevo León, Apodaca, Nuevo León 66600, México*

Received 30 June 2010; accepted 19 April 2011
DOI 10.1002/app.34725
Published online 23 August 2011 in Wiley Online Library (wileyonlinelibrary.com).

ABSTRACT: In this work, we report on the application of fractional calculus to the modeling of the isochronal behavior of complex magnetic susceptibility obtained from polymer–magnetic nanocomposites composed of cobalt-ferrite nanoparticles embedded into a chitosan matrix. From the isochronal measurements of real and imaginary parts of the complex magnetic susceptibility and temperature-dependent static measurements, performed at different applied dc-fields, it was observed that the spins' response is mainly leaded by three contributions, which are attributed to the intrinsic magnetic anisotropy of the particles, the surface-to-core spins exchange within particles and to the dipole-dipole interactions among particles. Accounting these contributions, the proposed magnetic model was capable to describe, in very precise way, the experimental behavior of both, real and imaginary, parts of the complex magnetic susceptibility, at temperatures below to that related to the transition of the polymer–magnetic nanocomposite into the superparamagnetic regime. © 2011 Wiley Periodicals, Inc. J Appl Polym Sci 123: 2154–2161, 2012

Key words: polymer–magnetic nanocomposite; cobalt-ferrite nanoparticles; chitosan; complex magnetic susceptibility; fractional calculus; fractional magnetic model

INTRODUCTION

Magnetic nanoparticles are an important class of advanced material, since its properties can be substantially modified from an appropriate size and morphology control. The magnetic properties of nanostructured materials differ from their bulk counterpart, because its magnetic order is confined to small crystalline domains, composed by a reduced amount of atoms or ions.[1] Thus, energetic balance between the magnetic anisotropy and magnetostatic energies among spins, favors the fact that the magnetic ordering of nanoparticles is based on single domains.[2] As a consequence, the change on its magnetization does not occurs by domains walls motion, instead it is necessary the coherent rotation of the arranged spins of nanoparticles, which leads to enhance its hysteretic characteristics.[1] Nevertheless, as particle size continues to decrease, spins become capable to thermally fluctuate, consequently, high temperature magnetic response of small single-domain particles can resembles a paramagnet.[3] This behavior is known as superparamagnetism and occurs above certain temperature, called blocking temperature (T_B), at which spins orientation relaxes to multiples metastables states at response times shorter than measurement time.[1,2]

In addition to the aforementioned characteristics, magnetic nanoparticles are capable to show deviations from ordered magnetic arrangement, due to the presence of a large amount of superficial atoms or ions.[4] Specifically, the studies of magnetic properties of ferrimagnetic nanostructures, such as spinel ferrites, have suggested the existence of a layer of disordered spins on the particles surface. Deviations of normal ferrimagnetic ordering at spinel ferrite nanoparticles have been attributed to incomplete coordination on surface cations or to broken bonds with its oxygen neighbors.[4–7] This situation leads to no colineal arrangement between surface spins and ferrimagnetically ordered spins at nanoparticles core, which has been suggested to be randomly canted.[8,9] Moreover, in systems with a high concentration of nanoparticles, interactions among particles can be significant, due to dipole–dipole interactions and exchange interactions among particles in close

Correspondence to: M. E. Reyes-Melo (mreyes@gama.fime.uanl.mx).

contact; both kinds of interactions are important sources of changes on the spins response. These interactions can favor either parallel or antiparallel orientation of spins, depending on particles morphology, magnetic anisotropy and its sizes.[4,10] Therefore, magnetic nanoparticles systems can depict analogous behavior to that showed by glassy magnetic materials (e.g., spin-glasses and diluted magnets), where surface-to-core interactions and interactions among particles can impose frozen magnetic states. This situation leads to deviations from the picture of single-domain particles as superspins with stable magnetic ordering.[4–10]

To describe how these interactions contributes to the magnetic response of a given nanoparticles system, studies about the energetic barrier over which spins relaxes emerge as good approaches.[4] Accordingly, the isochronal study of complex magnetic susceptibility, $\chi^* = \chi' - i\chi''$, is a powerful tool for the elucidation of how spins of nanoparticles relax under dynamic stimuli, given by an applied ac magnetic field.[11–13] Two typical magnetic relaxation mechanisms can be observed in nanoparticles systems, depending on the degrees of freedom of the spins to respond. For example, at polymer–magnetic nanocomposites, where nanoparticles find themselves stabilized into a matrix,[13,14] the relaxation of the nanoparticles spins occurs through Néel-relaxation, which can be describe by means of an Arrhenius-like formalism.[15] However, since the nanoparticles systems, specially the ferrimagnetic ones, show certain degree of surface-to-core exchange and particles interactions, they can display deviations from the Néel formalism, and the response of its spins could be describe assuming cooperative relaxation mechanism, such as that proposed by the Vogel-Fulcher law (VFL).[11–13,15]

Moreover, when the nanoparticles of a magnetic system have significant magnetic anisotropy energy, which blocks the internal reorientation of its spins, and the friction between particles and molecules of the dispersion media can be easily overcame (e.g., ferrofluids), nanoparticles can display diffusional rotation, to respond to external ac-field.[15–18] This relaxation mechanism is known as brownian-relaxation and takes place through the competition between viscosity of dispersion media and thermal fluctuations induced into the magnetic system.[17]

From dynamic magnetic measurements of χ^* is possible to study magnetic relaxation phenomena, because we can separate χ^* into its real and imaginary parts. The real part, χ', represents the component that is in-phase with the applied ac field, whereas the imaginary part, χ'', is proportional to the $\pi/2$ out-of-phase or quadrature component of dynamic magnetization. Hence, the imaginary component can be related to the dissipated energy by the magnetic system, whereas the real part is associated to partially stored energy.[14,19] For the interpretation of the experimental data of χ^*, it is necessary to use mathematical models due to the complexity of the dynamic magnetic properties of nanoparticles systems. In this sense, the use of differential and integral operators of fractional order is a good alternative, as has been reported elsewhere.[20]

The goal of this work is the application of fractional calculus to the modeling of isochronal complex magnetic susceptibility of a polymer–magnetic nanocomposite. Using this fractional magnetic model we attempt to describe the relaxation phenomena related to distinct sources that contribute to the magnetic response of polymer–magnetic nanocomposites. The proposed model will be validated using experimental data obtained from dynamic isochronal magnetic measurements of a reported polymer–magnetic nanocomposite, composed by cobalt–ferrite nanoparticles embedded into a chitosan matrix.[21]

MAGNETIC PROPERTIES OF CHITOSAN/COBALT–FERRITE NANOCOMPOSITE

Instrumentation

The isochronal complex magnetic susceptibility of the chitosan/cobalt-ferrite (CHN/CoF) nanocomposite was measured in a Quantum Design PPMS-9, after a zero field-cooled (ZFC) process, using an ac-field amplitude of 0.4 mT at frequencies of 10, 50, 100, 250, 500, 1000, 2500, 5000, and 10,000 Hz, in a temperature interval between 2 and 300 K. In addition, static magnetic measurements of temperature-dependent magnetization, $\sigma(T)$, were performed at different applied magnetic fields, using a Quantum Design MPMS SQUID-VSM magnetometer, in a temperature interval between 1.8 and 300 K.

Description of experimental complex magnetic susceptibility behavior

Figure 1 shows the experimental curves of the real part of the complex magnetic susceptibility, obtained from CHN/CoF nanocomposite. As one can notice, all curves display an increment on its magnitude as temperature increases, until they reach a maximum at a given temperature, T_M, from which all curves describe a decrease on its magnitude. To explain this behavior, it is necessary to divide these features into two regimes: one associated to a temperature interval below T_M, and another for temperatures above T_M.[4] At temperatures below T_M, the increment of the magnitude of the real part, as a function of temperature, can be explained as the thermally induced relaxation of spins over the energetic barrier imposed by the intrinsic magnetic anisotropy of the

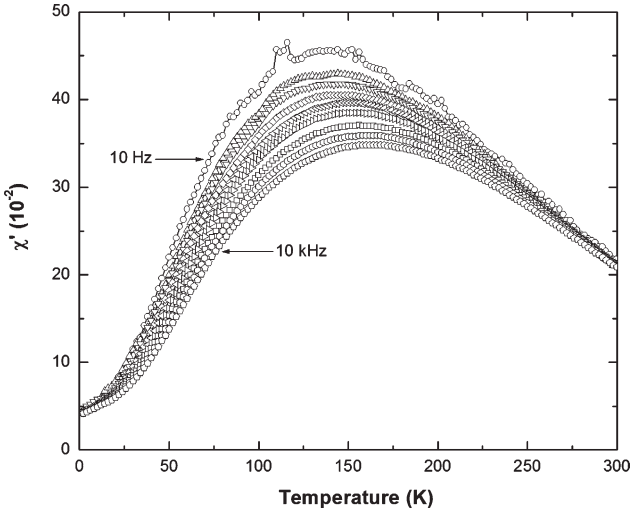

Figure 1 Isochronal behavior of real part of complex magnetic susceptibility obtained at 10, 50, 100, 250, 500, 1000, 2500, 5000, and 10,000 Hz from polymer–magnetic CHN/CoF nanocomposite.

particles. As temperature increases, the thermally induced fluctuations over the spins activate its response to the applied ac-field. This feature is also observed on the curves of the imaginary part, which describe an increment on its magnitude as temperature increases (see Fig. 2).

As temperature continue to increase, the curves of the real part display a significant change on its slope (see Fig. 1) at temperatures close to that associated to the maximum of its imaginary counterparts (see Fig. 2). This behavior can be explained as an increment on the population of relaxed spins as a function of temperature, which progressively becomes capable to partially store and dissipate the magnetic energy given from the applied ac-field. Thus, the temperature at which the maximum of the imaginary part occurs can be understood as the threshold for the relaxation of the entire spins of the CHN/CoF nanocomposite. Following this reasoning, once that the entire spins population relaxes, and they are capable to respond to the applied ac-field, one can expect that the real part reaches its maximum and its magnitude remains independent of temperature increment. However, as Figure 1 shows, such feature is not present in the curves of the real part; instead, the curves describe a decrease on its magnitude as temperature increases above T_M.

To explain the decrease on the magnitude of the curves of the real part (see Fig. 1) as temperature increases above T_M, it is necessary to elucidate the phenomenon at this temperature. As temperature reaches T_M, the entire spins population on the nanocomposite is able to respond to applied ac-field. Nevertheless, as temperature continues to increase above T_M, the thermal energy becomes greater than the magnetic energy given to the spins from the ac-field. This situation leads to instabilities on the spins reorientation, and eventually its response no longer follows the applied ac-field. Therefore, the phenomenon at T_M can be related to the transition of the magnetic system into the superparamagnetic regime. As it has been documented in the literature, when a magnetic nanoparticles system get into the superparamagnetic regime, its magnetic ordering is blurred by thermally induced fluctuations and its remanence vanishes.[1–4,22] Thus, is safe to argue that the decrease on the magnitude of the curves of the real part at temperature above T_M occurs due to the vanishing of the magnetic ordering on CHN/CoF nanocomposite.

Moreover, it is worth to mention that, as Figure 1 shows, the temperature at which the curves of the real part exhibit their maximum tends to increase as frequency increases, as well as they show a decrease on the magnitude of their maximum, which is proportional to the frequency increment. The shift on the curves maximum to higher temperatures as frequency increases corroborates that the blocking process at T_M is thermally activated. Furthermore, the decrease on the magnitude of their maximum as frequency increases seems to be related to the increment on the maximum of the curves of its imaginary counterparts (see Fig. 2). This increment can be explained as an increment of the portion of magnetic energy that is dissipated as frequency increases, since the time window associated to dynamic measurement becomes narrower and very close to the nanoparticles spins response time. This means that as frequency increases, the response time of

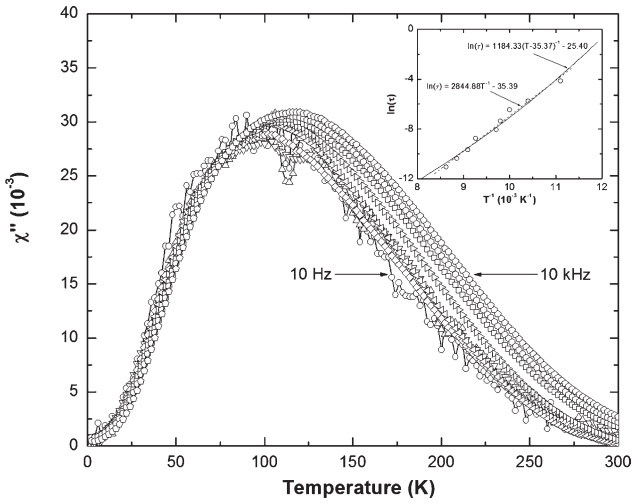

Figure 2 Isochronal behavior of imaginary part of complex magnetic susceptibility obtained at 10, 50, 100, 250, 500, 1000, 2500, 5000, and 10,000 Hz from polymer–magnetic CHN/CoF nanocomposite. Inset shows the evolution of maximum of imaginary part curves in a graph of ln(τ) versus T^{-1}.

nanoparticles spins become longer than the width of the time window of the dynamic measurement, hence the nanoparticles spins needs to reduce its response time to follow the applied ac-field and relax. Following this reasoning, the relaxation of spins on the CHN/CoF nanocomposite should begin at higher temperatures as frequency increases (see Fig. 1). Thus, it is possible to state that the response time of spins evolve and become shorter as temperature increases, which unequivocally indicates that its relaxation is thermally activated, and the relaxation mechanism could be describe by the Néel formalism.

To elucidate the manner that the spins relax, we proceed to analyze the evolution of the curves' maximum of the imaginary part in a graph of ln(τ) versus T^{-1} (see inset at Fig. 2), where τ represents the response time of the spins on CHN/CoF nanocomposite, and it can be related to the frequency (f) according to $\tau \approx (2\pi f)^{-1}$. As one can notice, the fitting given by the Néel formalism and that suggested by VFL, follow in close correspondence the experimental data of the evolution of the maximum on those curves. Nevertheless, the value of τ_0, obtained from the Néel formalism (4.3×10^{-16} s), lacks of physical meaning, suggesting significant particles interactions, which in addition to their intrinsic magnetic anisotropy, blocks the relaxation of its spins.[15] Accordingly, it is safe to argue that the relaxation process of spins is cooperative in nature, since it can be described as a collective response of an assembly of interacting particles, that found themselves blocked to relax due to its interactions at temperatures below T_0.[4,11,23–25] The magnitudes of the parameters obtained from the VFL fitting are: $E_A = 1.6 \times 10^{-20}$ J, $T_0 = 35.4$ K, and $\tau_0 = 9.3 \times 10^{-12}$ s. Furthermore, from these results, and considering the reported magnetic properties of the CHN/CoF nanocomposite,[21] the relaxation of its spins could be also leaded by a blocking process associated to disordered frozen spins layers on the CoF nanoparticles surface.[4,11,13] Thus, it is possible to assume that the relaxation of spins is mainly leaded by three contributions: intrinsic magnetic anisotropy of the particles, surface-to-core exchange, and particles interactions.

Elucidation of the contributions on the particles spins response

To elucidate the manner that each contribution leads the response of spins, we proceed to evaluate σ(T) at different applied dc-fields, measuring its ZFC and field-cooled (FC) static magnetic properties. It has been reported that from the study of temperature derivative of the difference between FC and ZFC magnetizations, $-d(\sigma_{FC} - \sigma_{ZFC})/dT(T)$, it is possible to obtain qualitative information regarding the relaxation processes on interacting particles magnetic systems.[26] Accordingly, Figure 3 shows $-d(\sigma_{FC} - \sigma_{ZFC})/dT(T)$ curves, obtained at the indicated dc-fields from CHN/CoF nanocomposite. As it can be noticed, the curve obtained from the measurement at 10 mT shows a maximum at $T_a = 6$ K. The maximum on this curve could be understood as the onset for the response of ordered spins in the nanoparticles. Moreover, a wide band with a maximum at $T_b = 47$ K can be also observed, which becomes narrower and shifts to lower temperatures as dc-field increases. This feature can be explained as follow.[26] At low temperatures, the population of spins is blocked to respond to the applied field. As temperature increases above T_a, the spins begin to thermally fluctuate and become able to respond to the applied dc-field. This situation contributes to increase the magnetization of the nanocomposite. In addition, as temperature approaches to T_b, the spins on the nanocomposite progressively overcome the energetic barrier that blocked its relaxation, and become free to respond to the applied field. This feature is observed as a difference on the magnitude of the maximum at T_b from that observed at T_a. Following this reasoning, the shift of the maximum at T_b suggest that as dc-field increases, the magnetic energy added to the nanocomposite polarize the surface-to-core exchange and the interaction among particles. Thus, is safe to argue that the band at T_b reflects a qualitative picture of the width of the energetic barrier over which the spins relax, since the width of this energetic barrier becomes narrower as the contributions from the surface-to-core exchange and particles interactions are blurred by its polarization. In such case, the magnetic ordering of spins on the nanocomposite

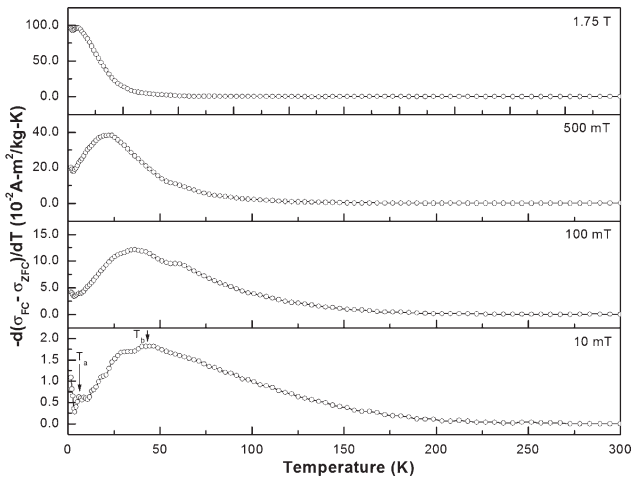

Figure 3 Graphs of the temperature derivative of the difference between FC and ZFC magnetization in function of temperature obtained at the indicated dc-field from polymer–magnetic CHN/CoF nanocomposite.

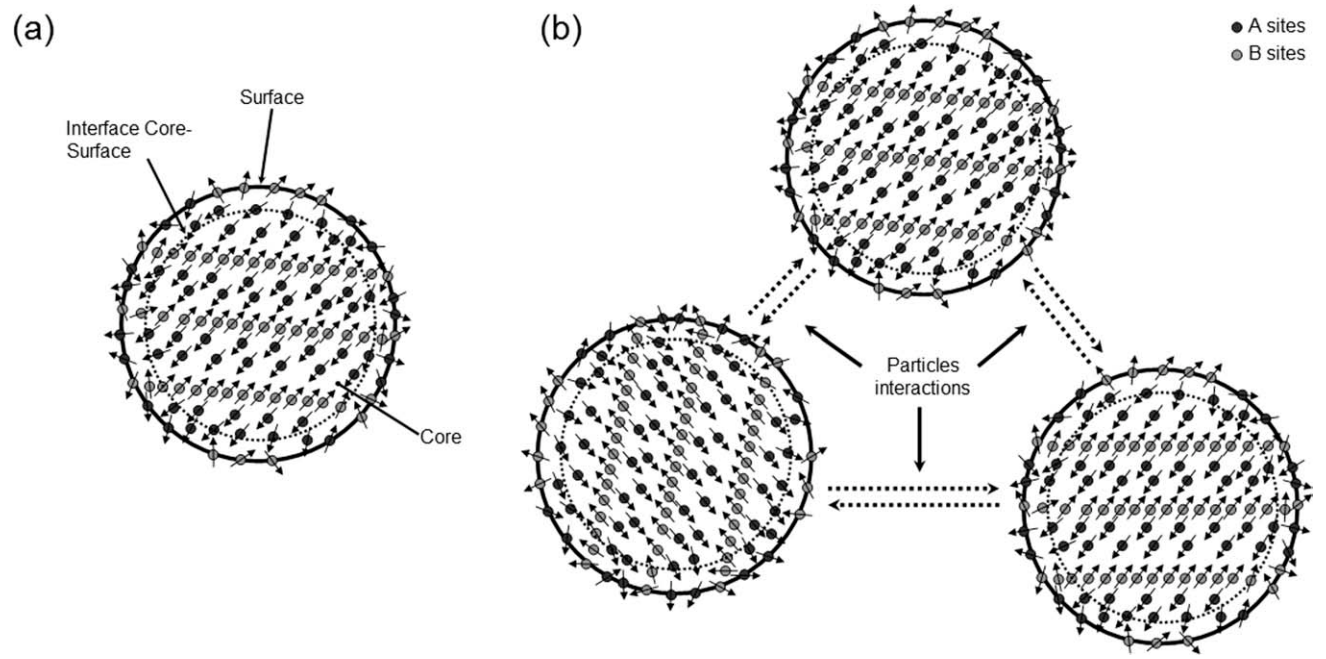

Figure 4 Schematic of (a) surface-to-core spins exchange and (b) dipole–dipole interparticle interactions that guide the magnetic response of polymer–magnetic CHN/CoF nanocomposite.

could be described as Figure 4 suggests. In Figure 4(a), the spins arrangement within CoF nanoparticles is illustrated, where a ferrimagnetic ordering at its core, which deviates to a randomly canted spins arrangement near to the nanoparticle's surface, can be noticed. In addition, Figure 4(b) shows a schematic of assembled nanoparticles due to dipole–dipole interactions. It is worth to mention that Figure 4 only represents a schematic picture elucidated from the observed magnetic behavior on this nanocomposite, although analogous spins arrangements have been previously calculated from finite element and Monte Carlo simulations for others magnetic systems of spinel ferrites nanoparticles.[4,27,28]

MODELING OF ISOCHRONAL COMPLEX MAGNETIC SUSCEPTIBILITY OF CHITOSAN/COBALT-FERRITE NANOCOMPOSITE

The fractional calculus and the resistor-inductor fractional element

The fractional calculus is the branch of mathematics that deals with the generalization of integrals and derivatives of real orders.[29] In this work we use a reported fractional element, which can perform an intermediary behavior between magnetic–inductor and electrical resistance.[20] This fractional element is called fractional resistor–inductor or FRI, and its constitutive equation can be expressed as:

$$V(t) = R\left(\frac{L}{R}\right)^{a}\frac{d^{a}I(t)}{dt^{a}} = R\tau^{a}D_{t}^{a}I(t) \;\text{ with }\; 0 \le a \le 1, \quad (1)$$

where $V(t)$ is the applied voltage, R and L are the electric resistance and magnetic inductance magnitudes, respectively, and $\tau = L/R$ is the characteristic response time, called relaxation time, which can be associated with the required time for the reorientation of particles' spins to a new equilibrium state. Finally, $D_t^a\ I(t)$ is the fractional derivate of the ath order of the electrical current with respect to time, which can be defined by the Riemann-Liouville derivative as:

$$D_{t}^{a}I(t) = D\int_{0}^{t}\frac{1}{\Gamma(1-a)}\frac{I(y)}{(t-y)^{a}}dy \;\text{ with }\; a \in (0,1), \quad (2)$$

where Γ is the Gamma function:

$$\Gamma(x) = \int_{0}^{\infty}\left(e^{u}u^{x-1}\right)du \;\text{ with }\; x > 0, \quad (3)$$

and "y" is a mathematical variable used in Riemann-Liouville derivative. The Riemann-Liouville equation is calculated from eq. (3), which is a fractional integral defined between 0 and time (t):

$$D_{t}^{-a}I(t) = \int_{0}^{t}\frac{1}{\Gamma(a)}\frac{I(y)}{(t-y)^{1-a}}dy \;\text{ with }\; a \in (0,\infty). \quad (4)$$

It is worth to mention that a fractional derivative [see eq. (2)] represents a convolution integral in which the function $I(t)$ is convolved with the impulse-response function of ath order. In this

context, eqs. (2) and (4) describe how a given state of a system is influenced by all states at earlier times. On another hand, from the physical point of view, the fractional order of a fractional integral [see eq. (4)] can be considered as an indication of the remaining energy in such system, given from a signal passing through it (e.g., signals given from mechanical, electrical, or magnetic stimuli). Furthermore, the fractional order of the fractional derivative reflects the rate at which a portion of the energy is dissipated by the system.

The constitutive equation of the FRI [see eq. (1)], is based on a differential operator of fractional order a, that can take values between 0 and 1.[20] From the FRI we can to obtain the behavior of an electrical resistance if $a = 0$, whereas for $a = 1$ it can be obtained the behavior of a magnetic inductor. Thus, for an interval of $0 < a < 1$, the FRI can display an intermediate behavior between the aforementioned limits.

In the next section we describe the application of the FRI element to the development of the proposed fractional magnetic model (FMM), which will be used to describe the behavior of the isochronal complex magnetic susceptibility of the polymer–magnetic nanocomposite, CHN/CoF. It is important to mention that, as one can deduce from the description given at this section, the use of fractional calculus for the conception of the FRI give us the opportunity to account for the distribution of relaxation times on the magnetic system, associated, for example, to particle size distribution, as has been successfully approached in the case of the dielectric manifestation of the viscoelasticity of polymer-dielectric materials.[30] Moreover, it can give information about the distribution of energy barriers over which the spins of the particles relax, and that can be related to contributions such as surface-to-core exchange and particles interactions, as has been reported elsewhere.[4]

Description of the fractional magnetic model

According to the experimental results, obtained from the static and dynamic magnetic measurements of the CHN/CoF nanocomposite, the use of three FRI elements, to develop the FMM, is proposed. Figure 5 shows the proposed FMM; constitutive equations of the employed elements are also showed in this figure. As it can be noticed, each of these FRI elements are considered into an array like the one showed in the dashed square. From each array we attempt to describe the contributions that lead the magnetic response of the CHN/CoF nanocomposite.

Applying the Fourier transform to the function $V(t)$, which is equal to the sum of the voltage droop on each array of the FMM, the complex inductance, L^*, of the model can be expressed as:

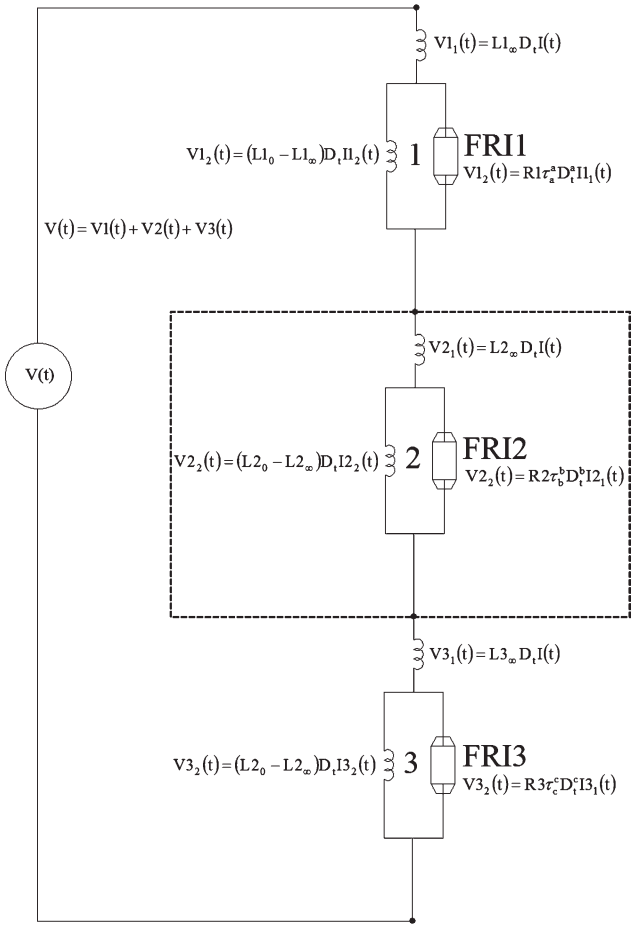

Figure 5 Fractional magnetic model proposed to describe the behavior of complex magnetic susceptibility of the polymer–magnetic CHN/CoF nanocomposite.

$$L^* = L1^* + L2^* + L3^* = (L1' - iL1'') + (L2' - iL2'') + (L3' - iL3''). \quad (5)$$

From the relation between the inductance and the magnetic susceptibility, $L = k(1 + \chi)$, where k is a constant which involves geometrical variables of the inductance, eq. (5) can be rewritten as:

$$\chi^* = \chi1^* + \chi2^* + \chi3^* = (\chi1' - i\chi1'') + (\chi2' - i\chi2'') + (\chi3' - i\chi3''), \quad (6)$$

where $\chi1^*$, $\chi2^*$, and $\chi2^*$ represents the complex magnetic susceptibility, described from the arrays 1, 2, and 3, respectively. From eq. (6), it is possible to obtain the mathematical expression for χ' and χ'' of the FMM:

$$\chi' = \chi1_\infty + \chi2_\infty + \chi3_\infty + \frac{(\chi1_0 - \chi1_\infty)(A_1 + A_2)}{(\omega\tau_a)^2 + 2A_2 + A_1} + \frac{(\chi2_0 - \chi2_\infty)(B_1 + B_2)}{(\omega\tau_b)^2 + 2B_2 + B_1} + \frac{(\chi3_0 - \chi3_\infty)(C_1 + C_2)}{(\omega\tau_c)^2 + 2C_2 + C_1}, \quad (7)$$

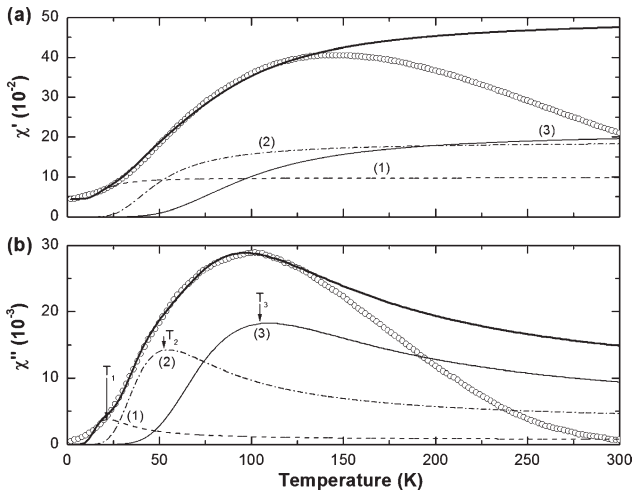

Figure 6 Description of the experimental data of (a) real and (b) imaginary parts obtained at 250 Hz by means of FMM theoretical curves (solid lines) as well as by the contributions (1), (2), and (3).

and

$$\chi'' = \frac{(\chi 1_0 - \chi 1_\infty)A_3}{(\omega\tau_a)^2 + 2A_2 + A_1} + \frac{(\chi 2_0 - \chi 2_\infty)B_3}{(\omega\tau_b)^2 + 2B_2 + B_1} + \frac{(\chi 3_0 - \chi 3_\infty)C_3}{(\omega\tau_c)^2 + 2C_2 + C_1}, \quad (8)$$

with: $A_1 = (\omega\tau_a)^{2a}$, $A_2 = (\omega\tau_a)^{1+a}\sin\left(\frac{a\pi}{2}\right)$, $A_3 = (\omega\tau_a)^{1+a}\cos\left(\frac{a\pi}{2}\right)$, $B_1 = (\omega\tau_b)^{2b}$, $B_2 = (\omega\tau_b)^{1+b}\sin\left(\frac{b\pi}{2}\right)$, $B_3 = (\omega\tau_b)^{1+b}\cos\left(\frac{b\pi}{2}\right)$, $C_1 = (\omega\tau_c)^{2c}$, $C_2 = (\omega\tau_c)^{1+c}\sin\left(\frac{c\pi}{2}\right)$, and $C_3 = (\omega\tau_c)^{1+c}\cos\left(\frac{c\pi}{2}\right)$.

Description of the experimental curves of complex magnetic susceptibility applying the FMM

To describe the experimental curves of the real and the imaginary parts of the complex magnetic susceptibility, measured from the CHN/CoF nanocomposite, we proceed to the modeling of the experimental data, from the evaluation of the eqs. (7) and (8). For this modeling, we selected the curves of the real and the imaginary parts measured at 250 Hz. It is worth to mention that there is not any special reason to select these curves, and they were selected only to exemplify the modeling of the experimental data using the proposed FMM. Figure 6 displays the experimental curves of the real and the imaginary parts, as well as the theoretical ones, obtained from the evaluation of eqs. (7) and (8); we also show the theoretical curves attributed to :(1) intrinsic magnetic anisotropy of the particles, (2) surface-to-core exchange at surface–core interfaces in the particles and (3) interactions among particles (see Fig. 4). It is important to mention that to evaluate the FMM we assumed that the response time of spins, τ, evolves following the Néel formalism, since the contributions that deviates the response of the particles to a cooperative relaxation have been already considered by the contributions associated to the arrays (2) and (3).

As Figure 6 shows, the theoretical curves of the real and imaginary parts are in good agreement with the experimental data of the complex magnetic susceptibility of the CHN/CoF nanocomposite. This result suggests that the parameters, used to model the experimental curves were properly selected. These parameters are summarized in the Table I. It is important to remark that the magnitude of the energy barrier attributed to the intrinsic magnetic anisotropy of the particles in this model is close to that expected for spinel ferrite nanoparticles systems without significant particles interactions.[15] Furthermore, the magnitude of the energy barriers related to the contributions described by the arrays (2) and (3) are close to that reported for cobalt ferrite nanoparticles systems with significant particle interactions[5]; the magnitudes of these energy barriers are also close to those obtained from the VFL fitting (see inset at Fig. 2).

Accordingly, the experimental data of the dynamic isochronal complex magnetic susceptibility of this nanocomposite can be described as follows. At low temperatures, energetic barriers imposed by contributions associated to arrays (1), (2), and (3) guide the orientation of the spins to be aligned on the direction of the particles easy axis, thus, its magnetic response is mainly leaded by its intrinsic magnetic anisotropy. As Figure 6(a) shows, the magnitude of the real part has a magnitude above zero, which suggests that the introduced magnetic energy (introduced as a form of work over the spins) is partially stored due to the random arrangement of easy axes of the particles. As temperature increases, the curve of the real part depicts a smooth inflection, which is quite well described by the theoretical curve obtained from the array (1), and can be understood as the relaxation of spins over the energetic barrier related to its intrinsic magnetic anisotropy; this feature is consistent with the magnitude of the exponent a obtained from the array (1) (see Table I). This inflection is also observed on the curve of the imaginary part, and as Figure 6(a) shows, can be associated to the maximum at $T_1 = 22$ K, which is

TABLE I
Values of the Parameters Used to Evaluate the FMM

Parameter	FMM elements		
	(1)	(2)	(3)
χ_∞	0.04	0.00	0.00
χ_0	0.10	0.20	0.23
E_A (J)	5.52×10^{-21}	1.19×10^{-20}	2.01×10^{-20}
τ_0 (s)	1×10^{-11}	1×10^{-10}	1×10^{-9}
a	0.83	0.82	0.80

displayed by the theoretical curve of the imaginary part obtained from the array (1).

Moreover, as Figure 6(a) shows, as temperature continues to increase, the curve of the real part describes a noticeable change on its slope, and rapidly increases its magnitude. This feature is related to the thermal activation of the spins of the particles, which become able to fluctuate and to respond to the applied ac-field. However, as temperature activates its fluctuation, spins on the surface of the particles deviate the response of the ferrimagnetically arranged ones in their cores [see the theoretical curve obtained from array (2)], increasing the magnetic energy that is dissipated by the nanocomposite; the magnitude of the exponent *a*, obtained from array (2), is in good agreement with this increment on the dissipated energy. The increment on the dissipated magnetic energy is corroborated by the increase on the magnitude of the imaginary part, as temperature increases above $T_2 = 53$ K [see Fig. 6(b)].

In addition, as temperature continues to increase above T_2, the slope of curve of the real part tends to decrease and eventually depicts a plateau-like feature [see Fig. 6(a)]. This behavior can be understood as the threshold for collective relaxation of the spins over the energetic barrier associated to the interaction among particles, since it occurs at temperatures near to that related to the maximum of the theoretical curve of the imaginary part, described by the array (3), at $T_3 = 105$ K [see Fig. 6(b)]; the magnitude of this maximum suggest that the quantity of the dissipated energy during this relaxation is larger than that observed on the aforementioned processes, which is in quite well correspondence with the value of the exponent *a*, obtained from the array (3). Thus, it is safe to argue that the cooperative relaxation of particles' spins is fully overcome at temperatures above 105 K.

Finally, as it can be noticed in Figure 6, at temperatures above T_M, the theoretical curves deviate from the experimental data of the real and imaginary parts. This deviation is attributed to the transition of the nanocomposite into the superparamagnetic regime, where thermally induced fluctuations overcome the magnetic work over the spins, which conduce to the vanishing of the magnetic order on the particles' assembly.

CONCLUSIONS

Using fractional calculus, as a mathematical tool, it was possible to describe the contributions that mainly guide the magnetic response of the studied polymer–magnetic CHN/CoF nanocomposite. Moreover, through the proposed FMM, it was also possible to elucidate the behavior of each contribution, from the assignation of each of it to a separate FMM array. Finally, it is worth to remark that from the definition of each array in the FMM, it is possible to establish that the order of fractional derivative could be considered as a relative measure of the partial dissipated or stored magnetic energy, which could be also associated to a given contribution.

References

1. Leslie-Pelecky, D. L.; Rieke, R. D. Chem Mater 1996, 8, 1770.
2. Kodama, R. H. J Magn Magn Mater 1999, 200, 359.
3. Unruh, K. M.; Chien, C. L. In Nanomaterials: Synthesis, Properties and Applications; Edelstein, A. S.; Cammarata, R. C., Eds.; Institute of Physics Publishing: London, 2002; Chapter 14.
4. Labarta, A.; Batlle, X.; Iglesias, O. In Surface Effects in Magnetic Nanoparticles; Fiorani, D., Ed.; Nanostructured Science and Technology Series, Spinger Science: Nueva York, 2005; Chapter 4.
5. López, J. L.; Pfannes, H.-D.; Paniago, R.; Sinnecker, J. P.; Novak, M. A. J Magn Magn Mater 2008, 320, e327.
6. Sato Turtelli, R.; Duong, G. V.; Nunes, W.; Grössinger, R.; Knobel, M. J Magn Magn Mater 2008, 320, e339.
7. Calero-DdelC, V. L.; Rinaldi, C. J Magn Magn Mater 2007, 314, 60.
8. Coey, J. M. D. Phys Rev Lett 1971, 27, 1140.
9. Gazeau, F.; Bacri, J. C.; Gendron, F.; Perzynski, R.; Raikher, Y. L.; Stepanov, V. I.; Dubois, E. J Magn Magn Mater 1998, 186, 175.
10. Martínez, B.; Obradors, X.; Balcells, L.; Rouanet, A.; Monty, C. Phys Rev Lett 1998, 80, 181.
11. Widatallah, H. M.; Al-Omari, I. A.; Sives, F.; Sturla, M. B.; Stewart, S. J. J Magn Magn Mater 2008, 320, e324.
12. Arelaro, A. D.; Lima, E., Jr.; Rossi, L. M.; Kiyohara, P. K.; Rechenberg, H. R. J Magn Magn Mater 2008, 320, e335.
13. Baldi, G.; Bonacchi, D.; Innocenti, C.; Lorenzi, G.; Sangregorio, C. J Magn Magn Mater 2007, 311, 10.
14. Vaishnava, P. P.; Tackett, R.; Dixit, A.; Sudakar, C.; Naik, R.; Lawes, G. J Appl Phys 2007, 102, 063914.
15. Novak, M. A.; Folly, W. S. D.; Sinnecker, J. P.; Soriano, S. J Magn Magn Mater 2005, 294, 133.
16. Erné, B. H.; Claesson, M.; Sacanna, S.; Klokkenburg, M.; Bakelaar, E.; Kuipers, B. W. M. J Magn Magn Mater 2007, 311, 145.
17. Fischer, B.; Huke, B.; Lücke, M.; Hempelmann, R. J Magn Magn Mater 2005, 289, 74.
18. Chung, S.-H.; Hoffmann, A.; Bader, S. D.; Liu, C.; Kay, B.; Makowski, L.; Chen, L. Appl Phys Lett 2004, 85, 2971.
19. Rosensweig, R. E. J Magn Magn Mater 2002, 252, 370.
20. Reyes, M. E.; Garza-Navarro, M. A.; González-González, V. A.; Guerrero-Salazar, C. A.; Martínez-Vega, J.; Ortiz-Méndez, U. J Appl Polym Sci 1943 2009, 112.
21. Garza-Navarro, M.; González-González, V. A.; Torres-Castro, A.; Hinojosa, M.; García-Loera, A.; José-Yacamán, M. J Appl Polym Sci 2010, 117, 785.
22. Ferreira da Silva, L. C.; Pereira, J.; Waerenborgh, J. C. J Non--Cryst Solids 2007, 353, 2374.
23. Shtrikman, S.; Wohlfarth, E. P. Phys Lett A 1981, 85, 467.
24. Matsuoka, S.; Hale, A. J Appl Polym Sci 1997, 64, 77.
25. Rault, J. J Non-Cryst Solids 2000, 271, 177.
26. Del Bianco, L.; Hernaldo, A.; Fiorani, D. In Surface Effects in Magnetic Nanoparticles; Fiorani, D., Ed., Nanostructured Science and Technology Series, Spinger Science: Nueva York, 2005; Chapter 7.
27. Kodama, R. H.; Berkowitz, A. E. Phys Rev B 1999, 59, 6321.
28. Kodama, R. H.; Berkowitz, A. E.; McNiff, J. E. J.; Foner, S. Phys Rev Lett 1996, 77, 394.
29. Cafagna, D. IEEE Indust Electron Mag 2007, 1, 35.
30. Reyes-Melo, M. E.; Martinez-Vega, J.; Guerrero-Salazar, C.; Ortiz-Mendez, U. J Appl Polym Sci 2006, 102, 3354.